Cellular Signalling 27 (2015) 394–401

Contents lists available at ScienceDirect

Cellular Signalling

journal homepage: www.elsevier.com/locate/cellsig

Active heat shock transcription factor 1 supports migration of the melanoma cells via vinculin down-regulation

Agnieszka Toma-Jonik, Wieslawa Widlak, Joanna Korfanty, Tomasz Cichon, Ryszard Smolarczyk, Agnieszka Gogler-Piglowska, Piotr Widlak, Natalia Vydra *

Maria Sklodowska-Curie Memorial Cancer Center and Institute of Oncology, Gliwice Branch, Wybrzeże Armii Krajowej 15, 44-101 Gliwice, Poland

ARTICLE INFO

Article history:
Received 16 September 2014
Received in revised form 23 October 2014
Accepted 6 November 2014
Available online 27 November 2014

Keywords:
Vinculin
Adhesion
Anchorage-independent growth
Metastasis
Thermotolerance

ABSTRACT

Heat shock transcription factor 1 (HSF1), the major regulator of stress response, is frequently activated in cancer and has an apparent role in malignant transformation. Here we analyzed the influence of the over-expression of a constitutively active transcriptionally-competent HSF1 mutant form on phenotypes of mouse and human melanoma cells. We observed that the expression of active HSF1 supported anchorage-independent growth *in vitro*, and metastatic spread in the animal model *in vivo*, although the proliferation rate of cancer cells was not affected. Furthermore, active HSF1 enhanced cell motility, reduced the adherence of cells to a fibronectin-coated surface, and affected the actin cytoskeleton. We found that although the expression of active HSF1 did not affect levels of epithelial-to-mesenchymal transition markers, it caused transcriptional down-regulation of vinculin, protein involved in cell motility, and adherence. Functional HSF1-binding sites were found in mouse and human *Vcl*/*VCL* genes, indicating a direct role of HSF1 in the regulation of this gene. An apparent association between HSF1-induced down-regulation of vinculin, increased motility, and a reduced adherence of cells suggests a possible mechanism of HSF1-mediated enhancement of the metastatic potential of cancer cells.

1. Introduction

Heat Shock Transcription Factor 1 (HSF1) is the major regulator of cellular response to stress, which is activated by various environmental and pathophysiological stimuli [2]. It is the primary transcriptional regulator of genes encoding for heat shock proteins (HSPs), which function as molecular chaperones and play an important role in the regulation of protein homeostasis and cell survival during proteotoxic stress. Moreover, HSPs mediate cytoprotection by the direct inhibition of key steps of programmed cell death [3]. Beyond the regulation of *HSPs* expression, HSF1 binds a broad array of non-*HSP* genes [18,29,37]. This property of HSF1 seems to be important in processes associated with development and growth [1,32], fertility [26,39,42], and longevity [30], which are not related directly with the HSF1-dependent regulation of HSPs.

A high level of HSF1 expression was observed in a broad range of cancer cell lines and human tumors including colorectal cancer, breast cancer, oral squamous cell carcinoma, hepatocellular carcinoma, multiple myeloma, and glioma [41]. Increased HSF1 expression has been associated with a reduction in the survival rate and was proposed as an independent prognostic factor for overall survival in patients with estrogen receptor-positive breast cancer [33] and hepatocellular carcinoma [8]. HSF1 could also change the sensitivity of cancer cells to cytotoxic treatment [15,40]. However, the specific role of HSF1 activity in malignant cells is not fully known. HSF1 is not a classical oncogene or tumor suppressor but rather interferes with many metabolic processes supporting tumor growth, which was called a "non-oncogene addiction" [35]. It was previously shown that HSF1 activation diminishes cell cycle checkpoints leading to aneuploidy [21] and influences RAS/MAPK and cAMP/PKA signal transduction pathways essential for malignant growth [7]. Furthermore, MEFs derived from *Hsf1*$^{-/-}$ animals were unable to form colonies in soft agar [16] and were deficient in migration induced by basal and epidermal growth factors [28]. The motility of bone marrow cells isolated from *Hsf1*$^{-/-}$ mice was also reduced [17]. The above-mentioned data suggests that HSF1 can affect the ability of cells to migrate. A high migration potential is thought to be a prerequisite for tumor cell invasion and spread, hence suggesting the involvement of HSF1 in the regulation of cancer metastasis. Importantly, HSF1 was found among six metastasis-promoting genes in malignant melanomas [34]. Its ability to promote migration and invasion was also observed in hepatocellular carcinomas [8]. Nevertheless, the exact

Abbreviations: EMT, epithelial to mesenchymal transition; HS, heat shock; HSF1, heat shock transcription factor 1; HSPs, heat shock proteins; MEFs, mouse embryonic fibroblasts

* Corresponding author at: Center for Translational Research and Molecular Biology of Cancer, Maria Sklodowska-Curie Memorial Cancer Center and Institute of Oncology, Gliwice Branch, Wybrzeże Armii Krajowej 15, 44-101 Gliwice, Poland. Tel.: +48 32 278 9679; fax: +48 32 278 9840.

E-mail addresses: agatoma5@wp.pl (A. Toma-Jonik), wwidlak@io.gliwice.pl (W. Widlak), joanna1540@op.pl (J. Korfanty), tcichon@io.gliwice.pl (T. Cichon), rsmolarczyk@io.gliwice.pl (R. Smolarczyk), agogler@io.gliwice.pl (A. Gogler-Piglowska), widlak@io.gliwice.pl (P. Widlak), nvydra@yahoo.co.uk (N. Vydra).

http://dx.doi.org/10.1016/j.cellsig.2014.11.029

role of HSF1 in the regulation of cancer cell growth and motility still remains unclear.

In this study, we aimed to determine the role of HSF1 in tumor growth and in the ability of cells to migrate. Melanoma cell lines (mouse B16F10 and human WM793B and 1205Lu) with modified levels of HSF1 activity were established and tested for different migration-related processes. We found that active HSF1 can support cell motility via a mechanism mediated by down-regulation of vinculin and an influence on the actin cytoskeleton organization.

2. Materials and methods

2.1. Experimental model

Melanoma cell lines: B16F10, WM793B and 1205Lu were purchased from the American Type Cell Culture Collection (ATCC, Manassas, VA). Cell culture and heat shock treatment were performed as described in details elsewhere [40].

2.2. DNA constructs and transfections

The aHSF1 (hHSF1ΔRD) construct, containing the active form of human HSF1 (with deletion of amino acid 221–315) driven by the human β-actin promoter, was kindly provided by Dr. A. Nakai [26]. The aHSF1 sequence was re-cloned into the pLNCX2 retrovirus expression vector (Clontech) downstream of the CMV promoter [14]. The target sequences for knock-down of mouse *Hsf1* gene were as follows: HSF1-1 (1856–1876, NM_008296.2)—5′ GCTGCATACCTGCTGCCTTTA; and HSF1-2 (341–359, NM_008296.2)—5′AGCACAACAACATGGCTAG. Stably transfected B16F10, WM793B and 1205Lu cells were obtained as described in details elsewhere [40].

2.3. Thermotolerance test

Logarithmically growing cells were thermally preconditioned by placing them in a water bath at a temperature of 42 °C for 1 h, then cells were allowed to recover in a CO_2 incubator at 37 °C for 6 h before a subsequent severe heat shock (1 h at 45 °C for B16F10 cells, 1 h at 48 °C for 1205Lu cells, or 30 min at 49 °C for WM793B cells). Alternatively, cells were subjected to a severe heat shock without preconditioning (condition of severe heat stress was established experimentally to achieve a cell survival rate which was higher than 50%). After heat shock cells were allowed to recover at 37 °C for 18 h, then harvested, stained with propidium iodide and analyzed on a FACS Canto cytometer (Becton Dickinson). Cell survival rate was calculated in relation to untreated controls; all experiments were performed in triplicate at least.

2.4. Proliferation test

Cells (2×10^4 cells per well) were seeded and cultured in 12-well plates. At the indicated time cells were washed with PBS, fixed in cold methanol, and rinsed with distilled water. Cells were stained with 0.1% crystal violet for 30 min, rinsed with distilled water extensively, and dried. Cell-associated dye was extracted with 1 ml of 10% acetic acid. Aliquots (200 μl) were transferred to a 96-well plate and the absorbance was measured at 595 nm (Synergy2, BioTek). Values were normalized to the optical density on day 0; all experiments were performed in triplicate at least.

2.5. Anchorage-independent growth

B16F10 cells (2×10^3 per well, in 1 ml of growth medium containing 0.35% noble agar, Difco, Becton Dickinson) were seeded on top of a solid growth medium containing 1% noble agar (1 ml) in a 12-well plate. Cells were covered with 300 μl of growth medium, which was supplemented every 3 days. After 21 days colonies were stained with 0.1% crystal violet and counted. All experiments were performed in triplicate at least.

2.6. Trans-well migration test (Boyden Chamber Assay)

Transwell chambers (with 8-μm pore size membrane, Becton Dickinson) were coated with fibronectin (10 μg/ml, Becton Dickinson). Cells (5×10^4 of B16F10 or 1205Lu, and 2.5×10^4 of WM793B) were suspended in a Hepes-buffered serum-free medium containing 0.1% BSA, seeded in the top of the chambers, and placed in the wells containing medium supplemented with 10% fetal bovine serum. After 4 h (B16F10 and 1205Lu) or 2 h (WM793B) the inserts were washed with PBS, fixed with cold methanol, rinsed with distilled water, and stained with 0.1% crystal violet for 30 min. The cells on the upper surface of the inserts were gently removed with a cotton swab. Cells that migrated onto the lower surface were counted under a microscope in five random fields; all experiments were performed in triplicate at least.

2.7. In vivo animal experiments

B16F10 cells (2×10^5 cells per mouse) were injected subcutaneously into 6–8-week-old C57BL/6 females (experimental group $n = 6$). Tumor growth was evaluated daily (for 8 days starting from tumor size ~10 mm^3) by caliper measurement in two perpendicular dimensions. Tumor volume was calculated using the formula: volume (mm^3) = 0.52 × (width)^2 × length [44]. To study the ability of B16F10 cells to metastasize, cells (2×10^5 cells per mouse) were injected into the tail vein (experimental group $n = 10$). Ten days after injection, mice were sacrificed by cervical dislocation. The lungs were collected and fixed in Bouin's solution. Metastasis foci were counted. All animal procedures were conducted in accordance with the recommendation of the Polish Council on Animal Care and were approved by the Local Committee of Ethics and Animal Experimentation at the Medical University of Silesia in Katowice, Poland (Decision No 77/2008 and 42/2012). The animals were maintained under controlled environmental conditions with a 1:1 light:darkness cycle, and were provided with unrestricted access to food and tap water.

2.8. Ki-67 index

Ki-67 immunostaining with polyclonal anti-rabbit antibody (1:1000; ab66155, Abcam) was performed on 5 μm-sections of paraformaldehyde-fixed (4% in PBS, overnight at 4 °C) and paraffin-embedded B16F10 tumors. An antigen retrieval step in 0.01 M citrate buffer pH 6.0 was performed before the immunohistochemistry procedure. An ImmPRESS Anti-Rabbit Ig (peroxidase) Polymer Detection Kit (Vector Labs, Burlingame, CA, USA) was used according to the manufacturer's guideline. DAB (3′,5′-diaminobenzidine) was used as a chromogen for visualization of immunohistochemical reactions and hematoxylin was used for nuclei counterstaining. Negative controls for specificity of the staining were performed by omitting the primary antibody. The Ki-67 index was determined by manual counting of >2000 cells from each section and shown as the relative number of nuclei showing positive staining.

2.9. RT^2 Profiler PCR array and quantitative RT-PCR

Expression of motility-related genes was assessed using the Mouse Cell Motility RT^2 Profiler PCR Array (SABiosciences, Frederick, USA). Total mRNA was isolated using a RNeasy kit (Qiagen) and converted into cDNA using a RT^2 First Strand Kit (SABiosciences, Frederick, USA). The cDNA was added to the RT^2 SYBR Green qPCR Master Mix (SABiosciences, Frederick, USA) and aliquotted on the Mouse Cell Motility PCR arrays. All steps, including analysis of PCR data, were carried out according to the manufacturer's protocol using the CFX96™ Bio-Rad Real-time System. Gene-specific quantitative RT-PCR was performed

using a Bio-Rad CFX 96™ Real-Time PCR Detection System. Forward and reverse primers (5 pmoles each) and cDNA template were added to Real-Time 2x PCR Master Mix SYBR A (A&A Biotechnology, Gdynia, Poland). Reactions were incubated at 95 °C for 3 min, followed by 40 cycles of 95 °C for 30 s, 58 °C for 30 s and 72 °C for 30 s. Analyzed genes were normalized against *GAPDH*. Primer characteristics used in analyses are presented in Suppl. Table 1.

2.10. Western blotting

Cellular proteins were extracted using a RIPA (Radio-Immunoprecipitation Assay) buffer, separated on 8–12% SDS-PAGE gels and electrotransferred onto a PVDF membrane (Merck Millipore). Primary antibodies used were: HSF1 (1:1000, ADI-SPA-901, Enzo Life Sciences), vinculin (1:1000, 05-386, Millipore), actin (1:3000, MAB1501, Millipore), HSC70/HSPA8 (1:3000, sc-7298, Santa Cruz Biotechnology), and antibodies from the EMT Antibody Sampler Kit (1:1000, #9782, Cell Signaling Technology). The primary antibody was detected by an appropriate secondary antibody conjugated with horseradish peroxidase (ThermoScientific), and visualized by an ECL (enhanced chemiluminescence) kit (ThermoScientific). When indicated, changes in the level of expression were estimated by protein bands densitometry using ImageJ software after normalization against loading controls (HSPA8 or actin).

2.11. Chromatin immunoprecipitation

Control cells (with the empty Neo vector) and cells expressing active HSF1 were trypsinized and suspended in 10 ml of CO_2 saturated media. For positive HSF1-binding probe, control (Neo) cells were heat shocked: an equal volume, pre-heated to 55 °C medium was added to the cell suspension, which immediately raised the temperature of the medium from 37 °C to 43 °C. The tube was submerged in a water bath at the 43 °C for an additional 15 min. Cells were fixed and the ChIP assay was carried out according to the protocol of ChIP kit of Upstate Biotechnology (Lake Placid, NY) using protein A-sepharose beads (Amersham). For 30 μg of chromatin sonicated to 100–500 bp fragments, 3 μg of rabbit anti-HSF1 (cat. no ADI-SPA-901, Enzo Life Sciences) polyclonal antibody was used. For ChIP negative controls chromatin samples were processed without antibody (mock IP). Immunoprecipitated DNA was dissolved in 20 μl of H_2O and analyzed by PCR (ChIP-PCR) using primers complementary to the *Hsph1*/*HSPH1* promoter (positive control of HSF1 binding) or to the *Vcl*/*VCL* gene sequences. For each reaction, 1 μl of the template was used and 40 PCR cycles were applied. In "Input" sample, 0.003–0.006% of the total material used in the ChIP assay served as the template for PCR. Primer characteristics used in analyses are presented in Suppl. Table 1.

2.12. Cell adhesion assay

96-well plates were coated overnight with 20 μg/ml of fibronectin (Becton Dickinson), and then blocked with BSA in a serum-free medium (rinsed twice with 0.1% BSA, blocked with 0.5% BSA for 60 min at 37 °C in a 5% CO_2 incubator then rinsed with 0.1% BSA). Cells (2×10^4 per well in 50 μl of medium with 10% of fetal bovine serum) were seeded into fibronectin/BSA-coated wells and into wells coated only with BSA (negative control), then allowed to attach for 30 min or 7 h. At the end of the experiment not adhered cells were removed by washing twice with serum-free medium containing 0.1% BSA and attached cells were fixed in 4% PFA for 10 min, and then stained with 0.1% crystal violet for 30 min, washed with water and air dried. Cell-associated dye was extracted with 200 μl of 10% acetic acid and absorbance was measured at 595 nm (Synergy2, BioTek). Relative adherence of cells was estimated as absorbance of cells adhered after 30 min vs. absorbance of cells adhered after 7 h (positive control), then percentage of cells adhered to BSA-coated cells was subtracted from values obtained in fibronectin-coated wells. All experiments were repeated four times at least; each repetition was represented by 8–12 wells.

2.13. Immunocytochemistry

Cells (5×10^4 per well) were seeded on 4-well glass slides (Nunc) coated with fibronectin (20 μg/ml, Becton Dickinson) and allowed to grow for 4 h. Then cells were briefly washed with PBS, fixed with 4% paraformaldehyde for 10 min, and permeabilized with 0.1% Triton-X100. After blocking with 2.5% normal goat serum, slides were incubated with an antibody against vinculin (1:100, 05-386, Millipore) at 4 °C overnight. The primary antibody was detected with a fluorescein isothiocyanate-conjugated secondary antibody (1:200, Sigma-Aldrich). Filamentous actin was visualized by incubation with tetramethylrhodamine B-conjugated phalloidin (1:800, Sigma-Aldrich), while nuclei were counterstained with DAPI (Sigma-Aldrich). Slides were mounted in a DAKO fluorescent medium (Dako), and analyzed under an Axioimager M2 microscope (Carl Zeiss, Germany) using a 63 X Plan Neofluar oil objective (NA = 1.25). Each experiment was performed in duplicate; approximately 200 cells were counted manually in randomly chosen fields for each duplicate.

2.14. Statistical analysis

For each dataset the normality of distribution was assessed by the Jarque–Bera test and homogeneity of variances was verified by the F— or Bartlett's tests depending on the subgroup number to provide optimal tools for statistical analysis; moreover, single outliers were identified by Dixon's test, while multiple outliers—by the Iglewicz–Hoaglin test. For analysis of differences between compared groups the quality of mean values was verified by the ANOVA test with pairwise comparison done with Dunnett's test. In case of non-Gaussian distribution, the Kruskal–Wallis ANOVA was applied for the verification of the hypothesis on the equality of medians with Dunn's test for pairwise comparisons. $P = 0.05$ was selected as a statistical significance threshold.

3. Results

3.1. Validation of the experimental model—expression of active HSF1 in melanoma cells is sufficient to develop thermotolerance

To mimic conditions of HSF1 activation in the absence of hyperthermia we established mouse (B16F10) and human (WM793B and 1205Lu) melanoma cells that over-expressed a constitutively-active transcriptionally-competent form of HSF1 (aHSF1) (Fig. 1A). In addition, we constructed B16F10 cells with silenced expression of HSF1 (using two different shRNAs: shHSF1-1 targeting 3′UTR, and shHSF1-2 targeting coding sequence). We have previously documented [40] that the aHSF1 could be effectively expressed in both mouse and human melanoma cells, which is accompanied with an increased expression of several inducible HSPs (HSPH1, HSPA1, HSPB1) already at physiological conditions (i.e. in the absence of hyperthermia). Furthermore, both HSF1-specific RNAi sequences diminished the *Hsf1* mRNA level, which was associated with the reduction of endogenous HSF1 protein level in B16F10 cells (Fig. 1A) and consecutive suppression of hyperthermia-inducible expression of *Hsph1*, *Hsp90aa1*, *Hspa1*, and *Hspb1* genes (shHSF1-1 targeting 3′UTR was more effective) [40].

To address the functional significance of active HSF1 level we assessed the survival of cells exposed to heat shock. Direct exposure of wild type cells (unmodified) or cells transfected with the empty vectors to severe heat shock (above 45 °C) caused a substantial reduction of cell survival in comparison to untreated control. Thermal preconditioning of such cells at the sublethal temperature (42 °C) resulted in a significant level of thermotolerance that protected them from subsequent severe heat stress. In contrast, the aHSF1-expressing cells exposed directly to severe heat shock showed a survival rate comparable

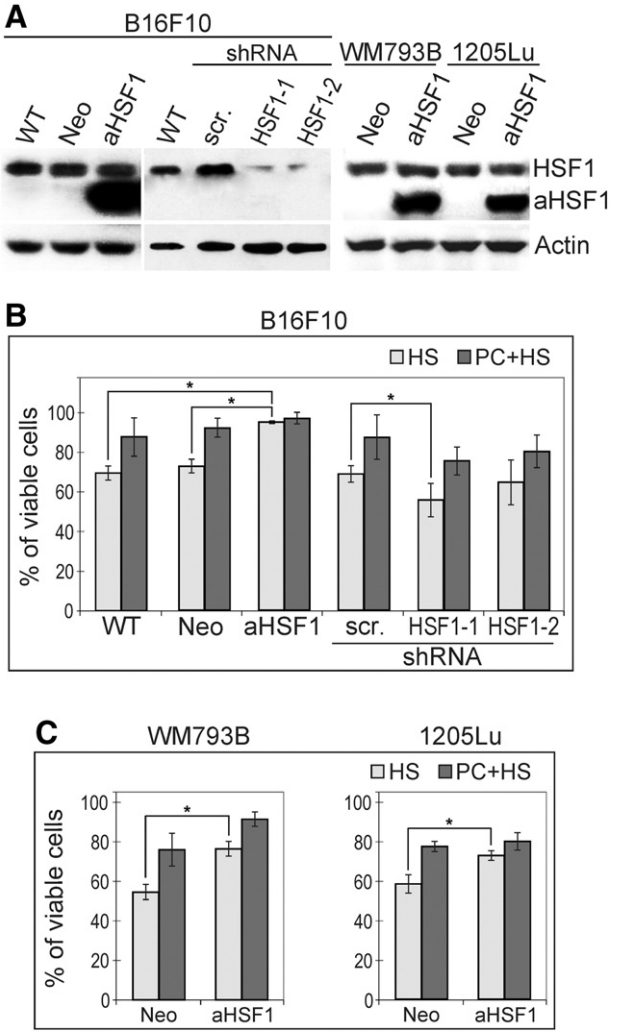

Fig. 1. Thermotolerance of mouse and human melanoma cells with different status of HSF1. (A) Western blot detection of HSF1 in B16F10, WM793B, and 1205Lu cells. Viability of mouse (B) and human (C) cells in different thermal conditions. The number of viable cells is depicted in relation to heat-untreated cells (100%). Untreated control—culture at 37 °C, HS—exposure to severe heat shock (above 45 °C); PC + HS—thermal preconditioning at 42 °C prior to severe heat shock. Cell description: WT—wild type, unmodified cells; Neo—control cells with the empty vector; aHSF1—cells over-expressing aHSF1; scr., HSF1-1, and HSF1-2—cells transfected with scramble shRNA, HSF1-1, and HSF1-2, respectively. The mean values and ±SD from at least three experiments are shown; asterisks represent *p*-values ≤0.05).

with the survival of preconditioned wild type cells (and preconditioning further increased the survival rate of such cells). The same result was observed for all three cell lines expressing aHSF1 (Fig. 1). Furthermore, B16F10 cells with silenced HSF1 were more sensitive to severe heat shock than wild type cells; the effect was stronger in the case of shHSF1-1 (Fig. 1B), which was more effective in silencing HSF1-dependent genes [40]. Thus, we have confirmed that the development of thermotolerance in melanoma cells depends on the activity of HSF1. We have also concluded that aHSF1 is able to regulate *HSP*s expression at a level sufficient to drive a thermotolerant phenotype; hence expression of aHSF1 in mouse and human melanoma cells mimics the conditions of HSF1 activation.

3.2. Expression of active HSF1 supports motility, anchorage-independent growth, and in vivo metastasis potential of melanoma cells

To assess the role of HSF1 in tumor growth we compared the proliferation rate of control B16F10 cells with a normal level of endogenous HSF1 (i.e., unmodified/wild type, or controls with the empty Neo vector or scramble shRNA) and cells with experimentally modified HSF1 level (i.e., with an over-expression of aHSF1 or HSF1 silenced by shRNA). We found that neither over-expression of aHSF1 nor silencing of endogenous HSF1 influenced the rate of cell proliferation *in vitro* and up to 72 h of culture no substantial differences between the tested cell lines were observed (Fig. 2A); the only exception was a slightly slower proliferation observed after 72 h in the case of shHSF1-2 silenced cells ($p = 0.023$). Similarly, neither expression of aHSF1 nor silencing of HSF1 affected cell proliferation *in vivo*—no significant differences in the growth of primary *in situ* tumors derived from B16F10 cells with a different HSF1 status injected subcutaneously into C57BL/6 mice were observed (Fig. 2B). Finally, we did not observe any significant differences in the pattern of Ki-67 proliferation marker between these tumors (Fig. 2C). We have concluded that neither activation nor inhibition of HSF1 influences the proliferation rate of B16F10 mouse melanoma cells.

In the next step we tested the influence of HSF1 status on the migration ability of B16F10 cells. We found that cells with over-expression of aHSF1 grow significantly faster in soft agar (anchorage-independent growth). Cells expressing aHSF1 generated two times more colonies ($p < 0.0001$; ANOVA test; Fig. 3A), and the colonies were markedly larger compared to control cells. However, the silencing of HSF1 did not affect the growth of cells in soft agar. Additionally, we tested the *in vitro* motility of cells using the Boyden chamber assay. We found

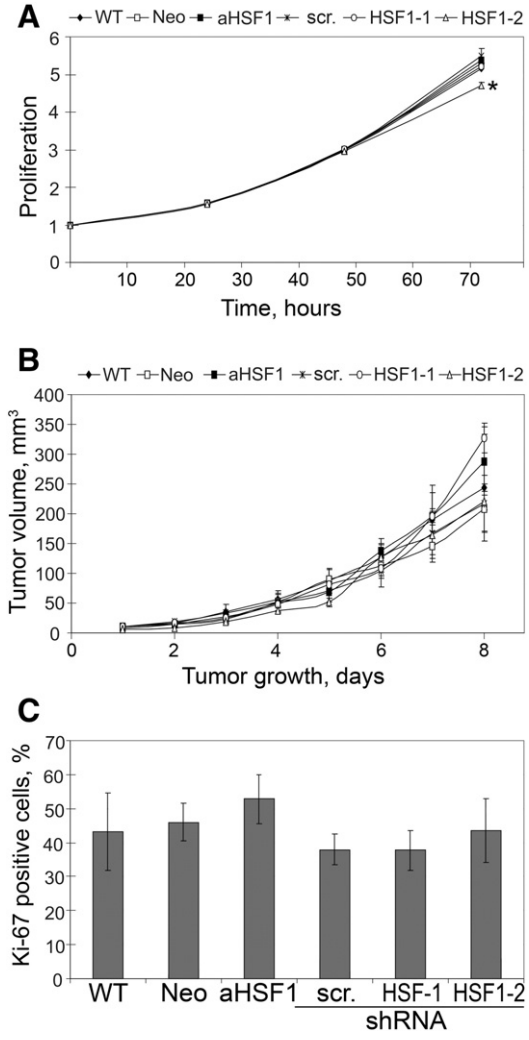

Fig. 2. Proliferation indices in B16F10 cells with different HSF1 status. (A) Cell growth *in vitro* (assessment based on crystal violet staining). (B) Volume of B16F10 tumors *in vivo*. (C) Ki-67 index in B16F10 tumors *in vivo*. The mean values and ±SD from at least three experiments are shown; an asterisk indicates $p < 0.05$. The description of cells is the same as in the Fig. 1 legend.

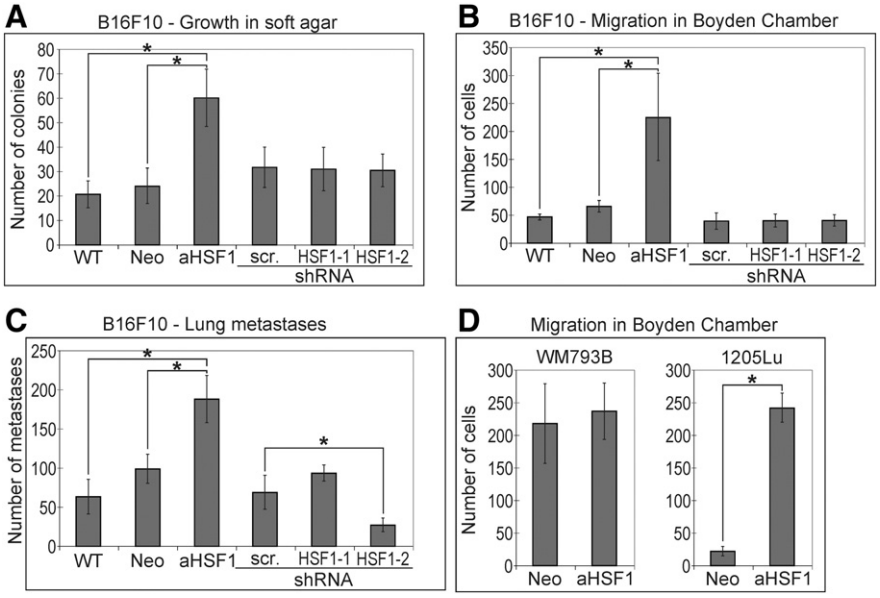

Fig. 3. Motility of cells with different HSF1 status. Anchorage independent growth in soft agar (A), migration in the trans-well chamber system (B), and the number of lung metastases *in vitro* (ten day after *iv* injection) (C) assessed for B16F10 cells with different HSF1 status. (D) Migration of WM793B and 1205Lu cells in the trans-well chamber system. The mean values and ± SD from at least three experiments are shown; asterisks indicate $p < 0.05$. The description of cells is the same as in the Fig. 1 legend.

that expression of aHSF1 significantly ($p < 0.0001$; ANOVA test) increased the potency of cells to migrate into the lower compartment of the chamber containing a medium with serum (Fig. 3B), yet silencing of HSF1 did not affect significantly this phenotype. Finally, we assessed the *in vivo* metastasis potential of B16F10 cells after their injection into the tail vein of C57BL/6 mice. The injection of cells with over-expression of aHSF1 led to the formation of a significantly higher number of lung metastases compared to mice injected with control cells ($p < 0.0001$; ANOVA test). Furthermore, the injection of cells with silenced HSF1 could result in a reduced number of lung metastases (the effect observed for line with HSF1-2 shRNA; $p = 0.019$) (Fig. 3C). We have concluded that the presence of active HSF1 supports the motility and metastatic potential of B16F10 mouse melanoma cells.

We tested also the ability of active HSF1 to support the motility of human WM793B and 1205Lu melanoma cell lines. We found that control WM793B cells showed a very high migration potential (in the Boyden chamber assay), which was barely enhanced by aHSF1 expression. In marked contrast, control 1205Lu cells showed a lower migration potential, which was significantly enhanced ($p = 0.0016$) in cells expressing aHSF1, resembling the effect observed in B16F10 cells (Fig. 3D). It should be noted that WM793B cells are of a pre-metastatic type and were established from the primary melanoma of a vertical growth phase, while 1205Lu cells are of a metastatic type and were derived from the lung metastases of WM793B cells. It is noteworthy, that in none of tested melanoma cell lines the expression of aHSF1 affected the ability to migrate in the scratch-wound assay (not shown).

3.3. Expression of active HSF1 reduces the level of vinculin

Increased cell migration is an *in vitro* functional marker of the epithelial to mesenchymal transition (EMT) [20], which frequently accompanies tumor progression and metastatic process. Knowing that expression of aHSF1 enhances migration potential we aimed to determine whether the status of HSF1 affects levels of EMT-associated proteins. We analyzed by Western blot levels of several EMT markers, including N-cadherin, E-cadherin, ZEB1, vimentin, catenin beta-1, SNAI1 (Snail1), SNAI2 (Slug), and claudin-1 (Fig. 4). None of the tested cell lines expressed E-cadherin (marker of epithelial cells) and claudin-1 (not shown), while N-cadherin was lacking in 1205Lu cells (derived from metastasis). Expression of SNAI1 and SNAI2 (which was not detected in B16F10 cells) was slightly decreased in WM793B and 1205Lu cells expressing aHSF1. However, other analyzed EMT markers were expressed at comparable levels irrespective of the HSF1 status in all cell lines. We have concluded that the HSF1-dependent enhancement of cell migration is not related to EMT up-regulation.

To further our search for possible migration-related factors targeted by HSF1, we used the Mouse Cell Motility RT^2 Profiler PCR Array to compare the expression of motility-related genes in control B16F10 cells and in cells over-expressing aHSF1. Among 84 analyzed genes we did not find any gene up-regulated due to the expression of aHSF1. However, the expression of several genes, namely *Vcl*, *Ptk2b*, *Cav1*, *Capn1*, and *Mmp2*, was significantly down-regulated ($p < 0.05$) in cells expressing aHSF1 (Fig. 5A). Human WM793B and 1205Lu cells over-expressing aHSF1 also showed a significant down-regulated level ($p < 0.05$) of *VCL* gene transcripts compared to control cells (Fig. 5B). In further studies we focused on the *Vcl* gene because at the protein level a significant down-regulation was observed only for vinculin when B16F10 cells expressing active HSF1 were analyzed. Moreover, a slightly increased

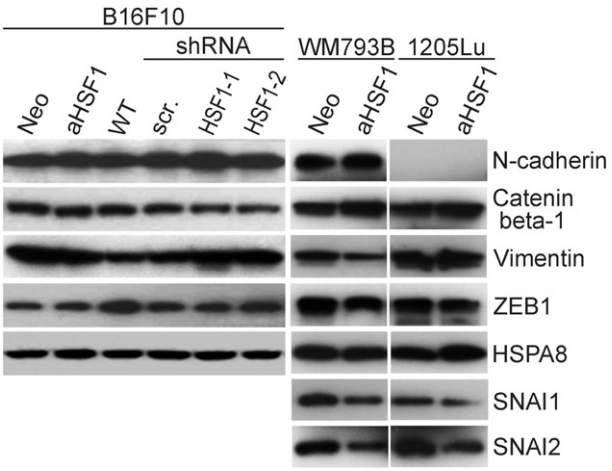

Fig. 4. Expression of the EMT markers in cells with different HSF1 status. Representative western blot analysis in B16F10, WM793B, and 1205Lu cells. HSPA8 was used as a loading control. The description of cells is the same as in the Fig. 1 legend.

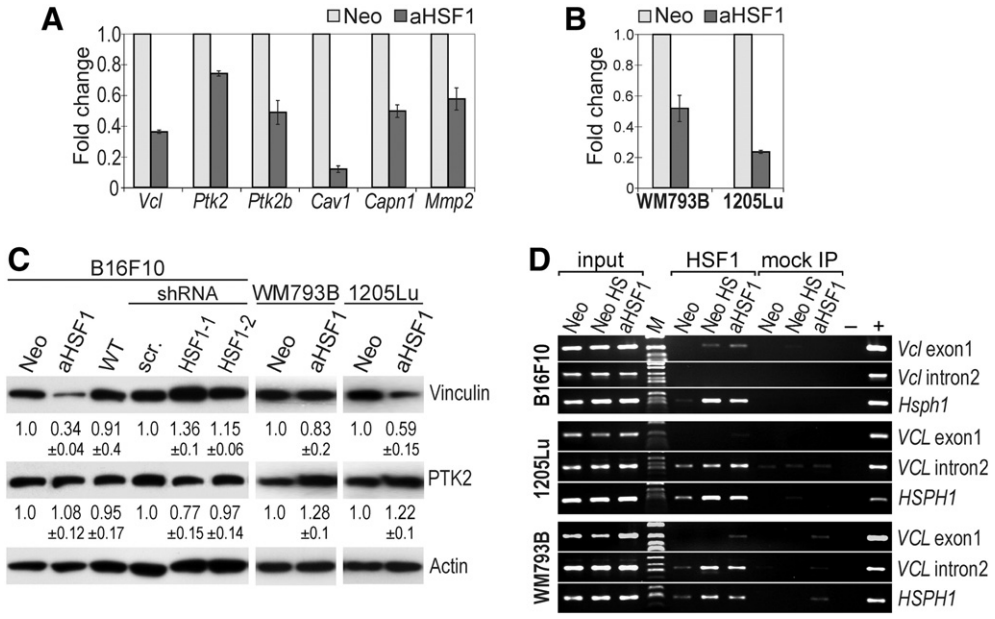

Fig. 5. Expression of vinculin in cells with different HSF1 status. Quantitative RT-PCR evaluation of mRNA level of motility-related genes in B16F10 cells (A) and *VCL* gene in WM793B and 1205Lu cells (B); shown are transcript levels in cells over-expressing aHSF1 in relation to Neo controls (for all differences p-value ≤ 0.05). (C) Western blot detection of vinculin and focal adhesion kinase (PTK2); actin was used as a loading control (shown are representative blots from three experiments). Numbers below blots represent protein ratios in relation to adequate controls (based on densitometry of three experimental repetitions, after normalization against actin). (D) Binding of HSF1 in the first exon and the second intron of *Vcl*/*VCL* gene analyzed by ChIP-PCR. *Hsph1*/*HSPH1* promoter was used as positive control for HSF1 binding. Mock IP—control reaction without Ab, −/+—negative and positive PCR control (without template/genomic DNA template). The description of cells is the same as in the Fig. 1 legend.

level of vinculin was detected in B16F10 cells with a down-regulated expression of HSF1 (line with HSF1-1 shRNA) (Fig. 5C). The level of vinculin protein was also down-regulated in 1205Lu cells but not in WM793B cells (Fig. 5C), which suggests an additional post-transcriptional mechanism of regulation in WM793B cells. The *VCL* gene contains several HSE motifs, which indicates the possible involvement of HSF1 in the gene regulation. Based on data of the HSF1 genome-wide binding assessed by ChIP-Seq in heat shocked U2OS cells (not published) we have chosen the potential HSF1 binding sites to be analyzed in melanoma cells. To directly confirm involvement of HSF1 in the regulation of the *Vcl*/*VCL* gene, an actual binding of HSF1 was assessed using ChIP assay. As expected, we found enhanced HSF1 binding to the promoter of the *Hsph1*/*HSPH1* gene (which is a typical target of HSF1) both in heat shocked cells and in cells expressing aHSF1 (Fig. 5D). In contrast, we did not identify HSF1 binding in the *Vcl*/*VCL* promoter in any melanoma cell lines (not shown). On the other hand, in the human *VCL* gene HSF1 binding was detected in the second intron, both in 1205Lu and WM793B cells. In the case of B16F10 cells binding of HSF1 was detected in the first exon (in both heat shocked and aHSF1-expressing cells), yet binding in the *Vcl* second intron was not detected (in any of six checked HSE-like motifs).

Most importantly, HSF1-mediated down-regulation of vinculin corresponded to cell migration ability analyzed *in vitro* using the Boyden chamber—in the same cells over-expression of aHSF1 resulted in the down-regulation of vinculin and increased motility. We have concluded that HSF1-dependent down-regulation of vinculin is associated with the enhanced ability to migrate in the case of B16F10 and 1205Lu cells.

3.4. Expression of active HSF1 affects the adhesion potential and the structure of the cytoskeleton of melanoma cells

Vinculin is a membrane-cytoskeletal protein present in focal adhesion plaques. Considering the HSF1-mediated down-regulation of vinculin we compared the ability of cells with different HSF1 status to adhere. The adhesion of cells to a fibronectin-coated surface and to a surface coated with BSA (considered as a non-adhesive protein) was compared. All tested cell lines adhered to fibronectin more effectively than to BSA: after the first 30 min of incubation significantly more cells were attached to the surface coated with fibronectin than to the surface coated with BSA. Most importantly, the expression of aHSF1 resulted in a reduced adhesion to fibronectin in the case of B16F10 ($p = 0.007$) and 1205Lu ($p = 0.17$) cells, while it did not affect the adhesion of WM793B cells (Fig. 6A). This result indicates an apparent association between the down-regulation of vinculin, the reduced adhesion and the enhanced motility of cells over-expressing active HSF1.

Considering interactions of vinculin with actin filaments [11] we analyzed the influence of aHSF1 expression on a structure of an actin cytoskeleton of melanoma cells. B16F10 cells growing on a fibronectin-coated surface were stained using an anti-vinculin antibody to visualize focal adhesion structures, and with fluorescent phalloidin to visualize actin filaments. We observed that the number of cells with focal adhesion structures was significantly reduced ($p < 0.0001$) in the population of cells over-expressing aHSF1 (Fig. 6B). We classified cells into three categories based on the morphology of the actin cytoskeleton: polarized (motile cells with a clear lamellipodium and trailing edge), ambiguous (multipolar cells with several lamellipodia), and not polarized (cells without lamellipodia). The status of HSF1 apparently affected distribution of cells among such defined categories: an underrepresentation of cells with polarized morphology ($p = 0.0006$) and an overrepresentation of cells with not polarized morphology ($p < 0.0001$) were observed in the population of cells over-expressing aHSF1 (Fig. 6C). This indicates the influence of HSF1-mediated mechanisms on the structure of the actin cytoskeleton of melanoma cells.

4. Discussion

HSF1 facilitates the malignant transformation and progression of cancer, yet detailed mechanisms of its pro-metastatic activity remain largely elusive. In the present work we used cells expressing a constitutively-active transcriptionally-competent form of HSF1 (aHSF1) [14,26,39,40] to study the influence of HSF1 activation on

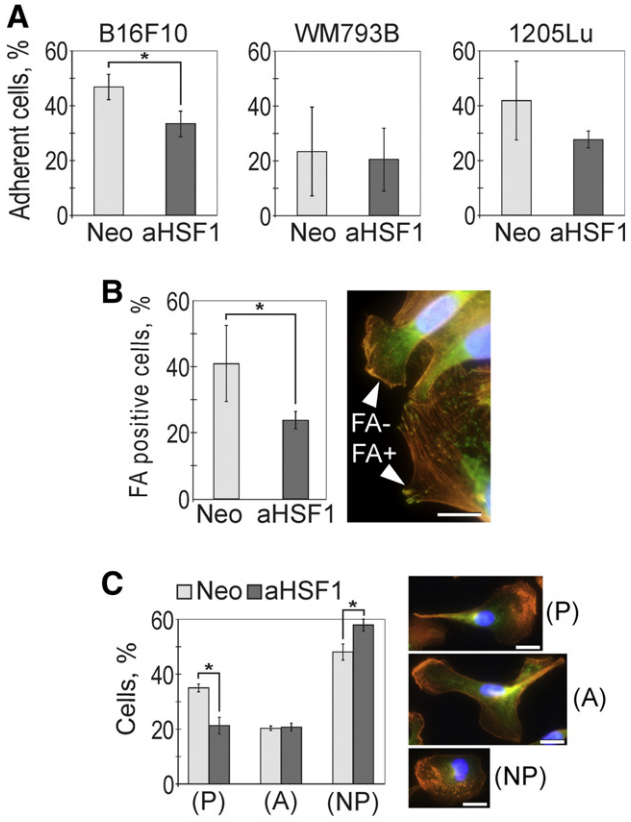

Fig. 6. Changes in adherence and morphology of cells with a different HSF1 status. (A) Adhesion potential of B16F10, WM793B, and 1205Lu melanoma cells; shown is relative adherence of cells to fibronectin-coated surface. (B) Focal adhesion (FA) structures in B16F10 cells over-expressing aHSF1; shown is the relative number of cells with focal adhesion structures (left), as well as an example of FA+ and FA− cells (right). (C) Relative numbers (left) and an example (right) of B16F10 cells with different morphologies: polarized (P), ambiguous (A), not polarized (NP). Red—actin cytoskeleton, green—vinculin, blue—nucleus. Scale bar—20 μm. Presented are mean values and ±SD from three experiments; asterisks indicate $p < 0.05$.

phenotype of cancer cells. We proved that the expression of aHSF1 allowed a developing thermotolerance in melanoma cells, resembling the function of endogenous heat-activated HSF1, which validated our experimental model. It has been previously suggested that HSF1 can support the growth of cancer cells [7]. However, we found that the expression of active HSF1 affects neither proliferation of melanoma cells *in vitro* nor the growth of corresponding tumors *in vivo*. Nevertheless, we found that the expression of active HSF1 enhanced the metastatic potential of mouse melanoma cells *in vivo*. Among the mechanisms critical for the formation of metastasis are cancer cell motility and anchorage-independent growth. Most interestingly, we found that the expression of active HSF1 affected both these features of cancer cells. Mouse B16F10 and human 1205Lu melanoma cells expressing active HSF1 acquired the enhanced migration ability when tested using the Boyden chamber assay. Because we did not observe a significant effect of HSF1 status in scratch assays, we concluded that HSF1 putatively affected chemotactic behavior. In the case of B16F10 cells we also found the enhanced ability of cells expressing active HSF1 to grow in soft agar (unattached to a surface). This indicates that the expression of active HSF1 promotes a loss of the contact inhibition and the anchorage independence, which are features of malignant transformation. Our observations were consistent with findings that down-regulation of HSF1 abrogated the ability of MEFs [28] or bone marrow cells [17] to migrate, while HSF1 overexpression could promote the migration of hepatocellular carcinoma cells [8]. An association of HSF1 expression with a metastatic potential was also described in prostate, hepatocellular, breast, colon and lung tumors [8,10,13,23,36]. Furthermore, it has been recently demonstrated that silencing HSF1 suppressed the migration and the invasiveness of human melanoma cells *in vitro*, and that HSF1 was required for melanoma invasion and metastasis, as well as tumorigenic potential *in vivo* [27]. All this data indicates collectively that HSF1 is involved in the regulation of cell migration and metastasis formation, although the specific mechanism of its action still remains unclear.

Cancer metastasis consists of several distinct steps, in which the epithelial–mesenchymal transition (EMT) and the mesenchymal–epithelial transition (MET) are critical events. The completion of the EMT is characterized by an increased capacity for migration and three-dimensional invasion [20]. It has been shown that hyperthermia enhanced cell migration and the EMT plasticity in lung A549 adenocarcinoma, but such stress-induced plasticity and migration was HSF1-independent [19]. Here we found that the expression of active HSF1 did not substantially affect the expression of several commonly used markers of EMT. Hence, the mechanism of HSF1-dependent stimulation of cell migration could be independent of EMT regulation. Cell migration is a complex process that integrates different protein–protein interactions and signaling events, and includes focalized adhesion dynamics and the remodeling of the structure of the actomyosin skeleton [9]. The potential role of HSPs and other chaperones in this process might be considered because they are involved both in functions of cytoskeleton [22] and metastasis [4,25,38]. Hence, we can not exclude that HSF1-regulated HSPs play a role in our experimental model. However, we found here that the expression of active HSF1 resulted in the down-regulation of several genes encoding for cytoskeleton proteins, including vinculin, which markedly expanded the range of HSF1-mediated mechanisms involved in metastasis. Vinculin localizes to integrin-mediated cell–matrix adhesion and cadherin-mediated cell–cell junction, and facilitates three-dimensional matrix invasion through up-regulation or enhanced transmission of traction forces [24]. MEFs deficient in vinculin showed a lower potential to spread, smaller focal adhesions and decreased strength of adhesion to fibronectin, laminin, vitronectin, and collagen, yet they migrated faster than their wild-type counterparts [43]. Lack of vinculin expression in MEFs or low vinculin expression in the mouse SV40 transformed 3T3 cells was associated with a higher cell motility and a greater ability to grow in soft agar [24,31,43]. Additionally, down-regulation of vinculin in mouse ovarian cancer cells was associated with a reduced number of focal adhesion and disorganized actin [6]. It was also reported that vinculin down-regulation led to enhanced invasiveness of human prostate cancer cells [5], and supported the cell motility of human colon adenocarcinoma Caco2 cells [12]. Hence, the level of vinculin is apparently associated with the enhanced motility of cells.

We found that the presence of active HSF1 resulted in the transcriptional down-regulation of vinculin. Furthermore, we evidenced actual binding of HSF1 in HSE/HSE-like motifs present in *Vcl*/*VCL* genes downstream of the transcription start sites (i.e. first exon or second intron). It has been observed that the binding of the HSF1 outside promoter is frequently associated with HSF1-mediated gene repression [23]. Hence, our data suggests the direct involvement of active HSF1 in transcriptional down-regulation of vinculin. Most importantly, we observed apparent association between HSF1-mediated down-regulation of vinculin, increased motility and reduced adherence of cells. Notable results were obtained with two closely related human melanoma cell lines: WM793B cells with basically high migration potential that was barely affected by active HSF1 and 1205Lu cells characterized by initially low migration potential that was largely increased by active HSF1 (similar to mouse B16F10 cells). Moreover, the expression of active HSF1 reduced the adherence of 1205Lu cells (similar to B16F10 cells), while initially the lower adherence of WM793B was not further reduced by active HSF1. Additionally, we found an unchanged level of vinculin in WM793B cells expressing active HSF1, in spite of the reduced level of *VCL* transcript, which suggests hypothetical post-transcriptional mechanisms of vinculin regulation in these cells (putatively not present in B16F10 and 1205Lu cells).

5. Conclusions

We concluded that the activation of HSF1 apparently enhanced the motility and metastatic potential of cancer cells, exemplified here by melanoma. Among potential HSF1-mediated mechanisms promoting cell motility and invasiveness we found transcriptional down-regulation of vinculin. Vinculin is a motility-related protein participating in the dynamic reorganization of the cytoskeleton and apparently playing important roles in the regulation of cell migration. Hence, HSF1-dependent down-regulation of vinculin offers a mechanistic explanation for HSF1-mediated enhancement of motility and metastatic potential of cancer cells.

Supplementary data to this article can be found online at http://dx.doi.org/10.1016/j.cellsig.2014.11.029.

Author contributions

AT-J: performed most experiments, analyzed data; WW: planned experiments, analyzed data, contributed reagents, prepared the manuscript; JK: performed ChIP experiments, contributed reagents; TC and RS: performed experiments with animals; AG-P: performed experiments; PW: prepared final version of the manuscript; and NV: planned and performed experiments, analyzed data, contributed reagents, prepared the manuscript.

Acknowledgments

The authors thank Dr. Akira Nakai for his generous gift of the hHSF1ΔRD (aHSF1) DNA, and Dr. Joanna Polańska for her assistance in statistical analyses. This work was supported by the Polish National Science Centre (Grant N401 031837 to NV and Grant 2011/03/N/NZ3/03926 to JK). All the calculations were carried out using GeCONiI infrastructure funded by project number POIG.02.03.01-24-099/13.

References

[1] M. Akerfelt, D. Trouillet, V. Mezger, L. Sistonen, Ann. N. Y. Acad. Sci. 1113 (2007) 15–27, http://dx.doi.org/10.1196/annals.1391.005.
[2] J. Anckar, L. Sistonen, Annu. Rev. Biochem. 80 (2011) 1089–1115, http://dx.doi.org/10.1146/annurev-biochem-060809-095203.
[3] S.K. Calderwood, M.A. Khaleque, D.B. Sawyer, D.R. Ciocca, Trends Biochem. Sci. 31 (2006) 164–172, http://dx.doi.org/10.1016/j.tibs.2006.01.006.
[4] C.-C. Chiu, C.-Y. Lin, L.-Y. Lee, Y.-J. Chen, Y.-C. Lu, H.-M. Wang, C.-T. Liao, J.T.-C. Chang, A.-J. Cheng, Clin. Cancer Res. Off. J. Am. Assoc. Cancer Res. 17 (2011) 4629–4641, http://dx.doi.org/10.1158/1078-0432.CCR-10-2107.
[5] K.R. Chng, C.W. Chang, S.K. Tan, C. Yang, S.Z. Hong, N.Y.W. Sng, E. Cheung, EMBO J. 31 (2012) 2810–2823, http://dx.doi.org/10.1038/emboj.2012.112.
[6] A.L. Creekmore, W.T. Silkworth, D. Cimini, R.V. Jensen, P.C. Roberts, E.M. Schmelz, PLoS ONE 6 (2011) e17676, http://dx.doi.org/10.1371/journal.pone.0017676.
[7] C. Dai, L. Whitesell, A.B. Rogers, S. Lindquist, Cell 130 (2007) 1005–1018, http://dx.doi.org/10.1016/j.cell.2007.07.020.
[8] F. Fang, R. Chang, L. Yang, Cancer 118 (2012) 1782–1794, http://dx.doi.org/10.1002/cncr.26482.
[9] P. Friedl, K. Wolf, Nat. Rev. Cancer 3 (2003) 362–374, http://dx.doi.org/10.1038/nrc1075.
[10] V.L. Gabai, L. Meng, G. Kim, T.A. Mills, I.J. Benjamin, M.Y. Sherman, Mol. Cell. Biol. 32 (2012) 929–940, http://dx.doi.org/10.1128/MCB. 05921-11.
[11] J. Golji, M.R.K. Mofrad, PLoS Comput. Biol. 9 (2013) e1002995, http://dx.doi.org/10.1371/journal.pcbi.1002995.
[12] S. Gu, N. Papadopoulou, O. Nasir, M. Föller, K. Alevizopoulos, F. Lang, C. Stournaras, Mol. Med. Camb. Mass 17 (2011) 48–58, http://dx.doi.org/10.2119/molmed.2010.00120.
[13] A.T. Hoang, J. Huang, N. Rudra-Ganguly, J. Zheng, W.C. Powell, S.K. Rabindran, C. Wu, P. Roy-Burman, Am. J. Pathol. 156 (2000) 857–864, http://dx.doi.org/10.1016/S0002-9440(10)64954-1.
[14] P. Janus, M. Pakuła-Cis, M. Kalinowska-Herok, N. Kashchak, K. Szołtysek, W. Pigłowski, W. Widlak, M. Kimmel, P. Widlak, Genes Cells Devoted Mol. Cell. Mech. 16 (2011) 1168–1175, http://dx.doi.org/10.1111/j.1365-2443.2011.01560.x.
[15] A.E. Kabakov, Y.V. Malyutina, D.S. Latchman, Radiat. Res. 165 (2006) 410–423.
[16] M.A. Khaleque, A. Bharti, D. Sawyer, J. Gong, I.J. Benjamin, M.A. Stevenson, S.K. Calderwood, Oncogene 24 (2005) 6564–6573, http://dx.doi.org/10.1038/sj.onc.1208798.
[17] M. Kubo, T.-S. Li, H. Kurazumi, Y. Takemoto, M. Ohshima, Y. Yamamoto, A. Nishimoto, A. Mikamo, M. Fujimoto, A. Nakai, K. Hamano, PLoS ONE 7 (2012) e37934, http://dx.doi.org/10.1371/journal.pone.0037934.
[18] M. Kus-Liśkiewicz, J. Polańska, J. Korfanty, M. Olbryt, N. Vydra, A. Toma, W. Widłak, BMC Genomics 14 (2013) 456, http://dx.doi.org/10.1186/1471-2164-14-456.
[19] B.J. Lang, L. Nguyen, H.C. Nguyen, J.L. Vieusseux, R.C.C. Chai, C. Christophi, T. Fifis, M.M. Kouspou, J.T. Price, Cell Stress Chaperones 17 (2012) 765–778, http://dx.doi.org/10.1007/s12192-012-0349-z.
[20] J.M. Lee, S. Dedhar, R. Kalluri, E.W. Thompson, J. Cell Biol. 172 (2006) 973–981, http://dx.doi.org/10.1083/jcb.200601018.
[21] Y.J. Lee, H.J. Lee, J.S. Lee, D. Jeoung, C.M. Kang, S. Bae, S.J. Lee, S.H. Kwon, D. Kang, Y.S. Lee, Oncogene 27 (2008) 2999–3009, http://dx.doi.org/10.1038/sj.onc.1210966.
[22] P. Liang, T.H. MacRae, J. Cell Sci. 110 (Pt 13) (1997) 1431–1440.
[23] M.L. Mendillo, S. Santagata, M. Koeva, G.W. Bell, R. Hu, R.M. Tamimi, E. Fraenkel, T.A. Ince, L. Whitesell, S. Lindquist, Cell 150 (2012) 549–562, http://dx.doi.org/10.1016/j.cell.2012.06.031.
[24] C.T. Mierke, P. Kollmannsberger, D.P. Zitterbart, G. Diez, T.M. Koch, S. Marg, W.H. Ziegler, W.H. Goldmann, B. Fabry, J. Biol. Chem. 285 (2010) 13121–13130, http://dx.doi.org/10.1074/jbc.M109.087171.
[25] G.M. Nagaraja, P. Kaur, A. Asea, Curr. Mol. Med. 12 (2012) 1142–1150.
[26] A. Nakai, M. Suzuki, M. Tanabe, EMBO J. 19 (2000) 1545–1554, http://dx.doi.org/10.1093/emboj/19.7.1545.
[27] Y. Nakamura, M. Fujimoto, S. Fukushima, A. Nakamura, N. Hayashida, R. Takii, E. Takaki, A. Nakai, M. Muto, Cancer Lett. 354 (2014) 329–335, http://dx.doi.org/10.1016/j.canlet.2014.08.029.
[28] C. O'Callaghan-Sunol, M.Y. Sherman, Cell Cycle Georgetown Tex 5 (2006) 1431–1437.
[29] T.J. Page, D. Sikder, L. Yang, L. Pluta, R.D. Wolfinger, T. Kodadek, R.S. Thomas, Mol. BioSyst. 2 (2006) 627–639, http://dx.doi.org/10.1039/b606129j.
[30] F.P. Perez, S.S. Moinuddin, Q. ul ain Shamim, D.J. Joseph, J. Morisaki, X. Zhou, Curr. Aging Sci. 5 (2012) 87–95.
[31] J.L. Rodríguez Fernández, B. Geiger, D. Salomon, A. Ben-Ze'ev, Cell Motil. Cytoskeleton 22 (1992) 127–134, http://dx.doi.org/10.1002/cm.970220206.
[32] W. Rupik, K. Jasik, J. Bembenek, W. Widłak, Comp. Biochem. Physiol. A Mol. Integr. Physiol. 159 (2011) 349–366, http://dx.doi.org/10.1016/j.cbpa.2011.04.002.
[33] S. Santagata, R. Hu, N.U. Lin, M.L. Mendillo, L.C. Collins, S.E. Hankinson, S.J. Schnitt, L. Whitesell, R.M. Tamimi, S. Lindquist, T.A. Ince, Proc. Natl. Acad. Sci. U. S. A. 108 (2011) 18378–18383, http://dx.doi.org/10.1073/pnas.1115031108.
[34] K.L. Scott, C. Nogueira, T.P. Heffernan, R. van Doorn, S. Dhakal, J.A. Hanna, C. Min, M. Jaskelioff, Y. Xiao, C.-J. Wu, L.A. Cameron, S.R. Perry, R. Zeid, T. Feinberg, M. Kim, G. Vande Woude, S.R. Granter, M. Bosenberg, G.C. Chu, R.A. DePinho, D.L. Rimm, L. Chin, Cancer Cell 20 (2011) 92–103, http://dx.doi.org/10.1016/j.ccr.2011.05.025.
[35] N.L. Solimini, J. Luo, S.J. Elledge, Cell 130 (2007) 986–988, http://dx.doi.org/10.1016/j.cell.2007.09.007.
[36] D. Tang, M.A. Khaleque, E.L. Jones, J.R. Theriault, C. Li, W.H. Wong, M.A. Stevenson, S.K. Calderwood, Cell Stress Chaperones 10 (2005) 46–58.
[37] N.D. Trinklein, J.I. Murray, S.J. Hartman, D. Botstein, R.M. Myers, Mol. Biol. Cell 15 (2004) 1254–1261, http://dx.doi.org/10.1091/mbc.E03-10-0738.
[38] S. Tsutsumi, K. Beebe, L. Neckers, Future Oncol. Lond Engl. 5 (2009) 679–688, http://dx.doi.org/10.2217/fon.09.30.
[39] N. Vydra, E. Malusecka, M. Jarzab, K. Lisowska, M. Glowala-Kosinska, K. Benedyk, P. Widlak, Z. Krawczyk, W. Widlak, Cell Death Differ. 13 (2006) 212–222, http://dx.doi.org/10.1038/sj.cdd.4401758.
[40] N. Vydra, A. Toma, M. Glowala-Kosinska, A. Gogler-Piglowska, W. Widlak, BMC Cancer 13 (2013) 504, http://dx.doi.org/10.1186/1471-2407-13-504.
[41] N. Vydra, A. Toma, W. Widlak, Curr. Cancer Drug Targets 14 (2014) 144–155, http://dx.doi.org/10.2174/1568009614666140122155942.
[42] W. Widłak, K. Benedyk, N. Vydra, M. Głowala, D. Scieglińska, E. Małusecka, A. Nakai, Z. Krawczyk, Acta Biochim. Pol. 50 (2003) 535–541 (doi:035002535).
[43] W. Xu, H. Baribault, E.D. Adamson, Dev. Camb. Engl. 125 (1998) 327–337.
[44] T. Cichoń, M. Jarosz, R. Smolarczyk, B. Ogórek, S. Matuszczak, M. Wagner, I. Mitrus, A. Sochanik, J. Jazowiecka-Rakus, S. Szala, Acta Biochim. Pol. 59 (2012) 377–381.